Article ID: 1003－6326(2005)03－0542－06

Preparation and magnetic properties of nanosized $(La_{0.47}Gd_{0.2})Sr_{0.33}MnO_3$ ①

WANG Gui(王 贵)[1, 2], WANG Zheng-de(王正德)[2], ZHANG Li-de(张立德)[2]
(1. College of Engineering, Zhanjiang Ocean University, Zhanjiang 524088, China;
2. Institute of Solid State Physics, Chinese Academy of Sciences, Hefei 230031, China)

Abstract: Nanosized $(La_{0.47}Gd_{0.2})Sr_{0.33}MnO_3$ perovskite oxides were prepared at relatively low calcinating temperature of 600 ℃ and 800 ℃ for 10 h using amorphous complex precursor. Curie temperature (T_c) and magnetocaloric effects(MCE) were investigated. X-ray diffraction(XRD) and electron diffraction(ED) reveal that the resulting products are of pure single-phase rhombohedral perovskite structure. Transmission electron microscopy (TEM) observation finds that the particle sizes are about 40－50 nm and 80－100 nm, and the T_c are 285.1 K and 285.9 K, MCE are about 2.02 J/(kg·K^{-1}) and 3.90 J/(kg·K^{-1}) at 5 T magnetic field. A relatively large MCE with a broad peak around Curie temperature is observed in sample sintered at 800 ℃ for 10 h. This suggests that nanosized $(La_{0.47}Gd_{0.2})Sr_{0.33}MnO_3$ is a suitable material as working substance in magnetic refrigeration in room temperature.

Key words: chemical synthesis; nanostructure materials; magnetocaloric effect; magnetic entropy change; perovskite manganite

CLC number: O 469 **Document code:** A

1 INTRODUCTION

The magnetic property and crystal structure of perovskite-type lanthanum manganese oxides were first studied by Jonker and Van Santen in 1950[1]. These materials were of considerable interest in the last decade due to their colossal magnetoresistance (CMR) effect[2-4]. Recently a series of hole-doped perovskite manganese oxides were reported to display a large magnetocaloric effect(MCE) in the vicinity of the ferromagnetic Curie temperature (T_c)[5-16], which may be exploited to be applied in magnetic refrigerator and heat pumps[17]. Ideal magnetocaloric material must exhibit an appreciable MCE in reasonably magnetic field. Meanwhile, they should be light in mass, and have good chemical stability, low-cost and nontoxic. In terms of the application in the magnetic refrigeration, a material that exhibits a flat MCE peak with applied magnetic field H in response to operation temperature range is needed[18]. These requirements may be met in the perovskite-type lanthanum manganese oxides, and their magnetic properties, Curie temperature and saturation magnetization can be tuned by either La-site or Mn-site element substitution. These materials are believed to be good candidates for magnetic refrigeration in various temperature ranges.

The properties of perovskite-type lanthanum manganese oxides obtained by various preparation methods are different[19-21]. Furthermore, nanosized material has been predicted to provide some new features in the MCE and magnetic properties comparing to the bulk material[22, 23]. The bulk polycrystalline samples of perovskite-type manganese oxides are usually prepared by conventional solid-state reaction method that needs higher temperature(1 000－1 600 ℃) and long annealing time to obtain homogeneous composition and desired structures. Sol-gel method has been widely used to prepare nanosized materials, and some excellent work has been done by Sanchez et al[24, 25], but it is limited by the stability of its precursor and its difficulty in doping different components of multi-metal ions in complicated systems. In this paper, a new method was used to prepare the nanosized $(La_{0.47}Gd_{0.2})Sr_{0.33}MnO_3$ at relatively low calcinated temperature, and its magnetism and MCE were studied. The reason of choosing Gd as the doping element is that Gd^{3+} has the largest spin among the rare-earth elements so that additional large magnetic entropy contribution from Gd^{3+} could be expected.

2 EXPERIMENTAL

Firstly, $La_2(CO_3)_3 \cdot 3H_2O$, $Gd_2(CO_3)_3 \cdot$

① **Foundation item:** Projects(50172048; 10374090) supported by the National Natural Science Foundation of China; Project(2002Z020) supported by the Talent Foundation of Anhui Province; Project(01044906) supported by the Science Foundation of Anhui Province, China
Received date: 2004－08－02; **Accepted date:** 2004－12－14
Correspondence: WANG Gui, Professor; Tel: +86-759-2362493; E-mail: zjwanggui@yahoo.com.cn

$3H_2O$, $SrCO_3$ and $MnCO_3$ powders (Grade: AR) with the desired molar ratio of La: Gd: Sr: Mn= 0.47: 0.2: 0.33: 1 were dissolved in pure water, then the excessive H_5DTPA (diethylene-triamine-pentaacetic acid) was added to the mixture. The above mixture was stirred and heated to about 80 ℃ to promote the dissolution and reaction. After the mixture became a transparent solution, it was filtered and then dried slowly at 60 ℃ until a piece of transparent glasslike material formed. Finally, the complex precursors were obtained after the solutions were dried completely at room temperature. The resulted complex precursors were annealed in the air at 600 ℃ and 800 ℃ for 10 h, respectively.

The thermogravimetric analysis (TGA) and differential thermal analysis (DTA) were performed by Shimadzu-50 and the heating rate was 10 ℃/min. The phase identification and structural analysis were carried out in X'Pert Pro MPD with Cu K_α radiation (λ= 0.154 18 nm). High-purity silicon powder was used as an internal standard to determine the lattice parameter. The morphology and particle size distributions were determined by Hitachi H-800 transmission electron microscopy (TEM) with accelerating voltage of 200 kV. The field cooling (FC) with field of 7 957.8 A/m and zero field cooling (ZFC) magnetization curve (M—T) as well as isothermal magnetization (M—H) curve were measured by Quantum Design Superconducting Quantum Interference Device MPMS System.

3 RESULTS AND DISCUSSION

3.1 Thermal decomposition of complex precursor

The thermal analysis results of TGA and DTA for the complex precursor are shown in Fig. 1. With the increasing temperature, there are mainly three mass loss regions in the TGA curve. According to quantity calculation of the mass loss in each region, the whole thermal decomposition process can be distinguished. The mass loss region from 20 ℃ to about 210 ℃ results from the loss of coordinated and solvent water. The region of mass loss from 230 ℃ to about 360 ℃ is due to the decomposition of CH_X organic components and amino-groups. The strong mass loss region from 360 ℃ to about 460 ℃ is related to the complete decomposition of the carboxyl metal group. The decomposition temperatures for the four kinds of carboxyl metal groups in such a precursor are very close, which is quite helpful to promote the formation of $(La_{0.47}Gd_{0.2})Sr_{0.33}MnO_3$.

The DTA result of the complex precursor shows a weak endothermic region below 210 ℃ and three exothermic peaks in the curve. The endothermic peak at 130 ℃ results from the loss of coordinated water. The peaks at 320 ℃ and 365 ℃ are produced by the decomposition of CH_X organic components and amino-groups. The exothermic peak at 445 ℃ is very strong, which contains both the exothermic contribution from the decomposition of carboxyl metal groups and the formation of the $(La_{0.47}Gd_{0.2})Sr_{0.33}MnO_3$ oxide.

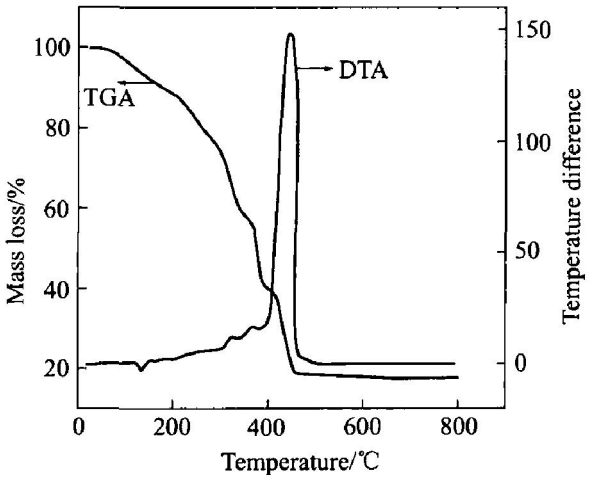

Fig. 1 TGA and DTA curves of complex precursor

3.2 Crystallization of nanosized $(La_{0.47}Gd_{0.2})Sr_{0.33}MnO_3$

According to the thermal analysis results of TGA and DTA for the complex precursor, sintered the precursor in the air at 600 ℃ and 800 ℃ for 10 h, respectively. The X-ray diffraction patterns of the precursor and the sintered samples at different temperatures are shown in Fig. 2. The precursor is amorphous. After the precursor is calcinated at 600 ℃ for 10 h, characteristic peaks of crystalline phase appear on the XRD pattern, which are indexed to pure rhombohedral perovskite-type crystal structure (space group $R\bar{3}C$), the lattice parameters are calculated by the Lapod program of Cohen's method[26], and the results are a= 0.546 4 nm and c= 1.347 0 nm. This indicates that $(La_{0.47}Gd_{0.2})Sr_{0.33}MnO_3$ with pure perovskite structure can be synthesized by this method even at relatively low calcinated temperature of 600 ℃.

The particle-sizes and morphologies of $(La_{0.47}Gd_{0.2})Sr_{0.33}MnO_3$ at different calcinated temperatures were examined by TEM, as shown in Fig. 3. When the precursor is calcinated at 600 ℃ for 10 h, the particle-sizes are about 40 – 50 nm (Fig. 3(a)), and the electron diffraction (ED) (inset in Fig. 3 (a)) indicates that the polycrystalline perovskite-type oxide is crystallized perfectly. As the calcinated temperature increases to 800 ℃, the particle size grows up to about 80 – 100 nm (Fig. 3(b)). TEM images show that the particles tend to aggregate with one another. These results indicate that the

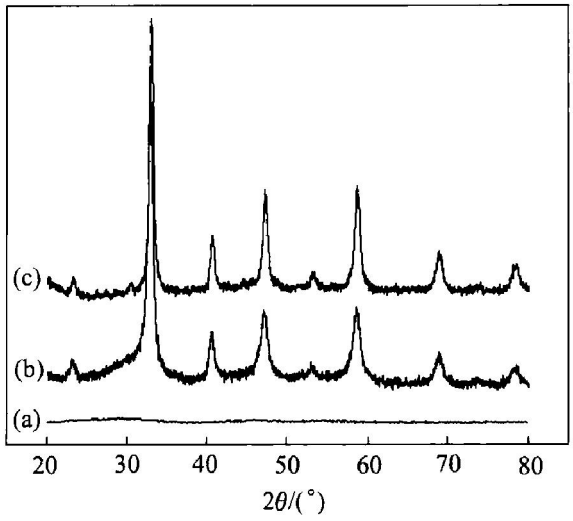

Fig. 2 XRD patterns of complex precursor and $(La_{0.47}Gd_{0.2})Sr_{0.33}MnO_3$ sample at different calcinating temperatures
(a) —Precursor; (b) —600 ℃, 10 h; (c) —800 ℃, 10 h

calcinating temperature has great effect on the particle size.

3.3 Magnetic properties and magnetocaloric effect of nanosized $(La_{0.47}Gd_{0.2})Sr_{0.33}MnO_3$

Fig. 4 shows the low-field(7 957.8 A/m) magnetization as a function of temperature in both zero-field-cooled(ZFC) and field-cooled (FC) processes for the samples calcinated at 600 ℃ and 800 ℃ for 10 h, respectively. The ferromagnetic Curie temperature is 285.1 K and 285.9 K respectively, for both samples, which is determined by a minimum in dM/dT curves as shown in Figs. 4(b) and 4(d). Comparing with the results by TEM, it can be found that the Curie temperature does not depend on the particle size. However, the magnetic ordering transition, as indicated by the derivative of the magnetization with respect to temperature dM/dT, becomes broader in the case of smaller particles. This result may be related to the larger surface and interface of smaller particles. The fact that Curie temperature of both samples decreases to near room temperature with the substituting rare-earth Gd may attribute to the crystallographic distortion induced by the smaller ionic radius of the substituting rare-earth ions. On the one hand, Gd^{3+} has a large local moment, and Gd doping may lead to the rise of Curie temperature and the strengthening of the magnetization. On the other hand, the crystallographic distortion induced by Gd doping may cause the decrease of Curie temperature and the magnetization. The ionic radius of La^{3+} is 0.1 032 nm, and the ionic radius of Gd^{3+} is 0.093 nm[27], so, the substitution leads to a decrease of the Mn—O bond distances and Mn—O—Mn bond angles, and results in a smaller double exchange interaction between Mn ions. The result of the experiments show the decrease of T_c and the magnetization is mainly dominated by the crystallographic distortion.

Based on the thermodynamical theory[28], the magnetic entropy change $\Delta S_M(T, H)$ associated

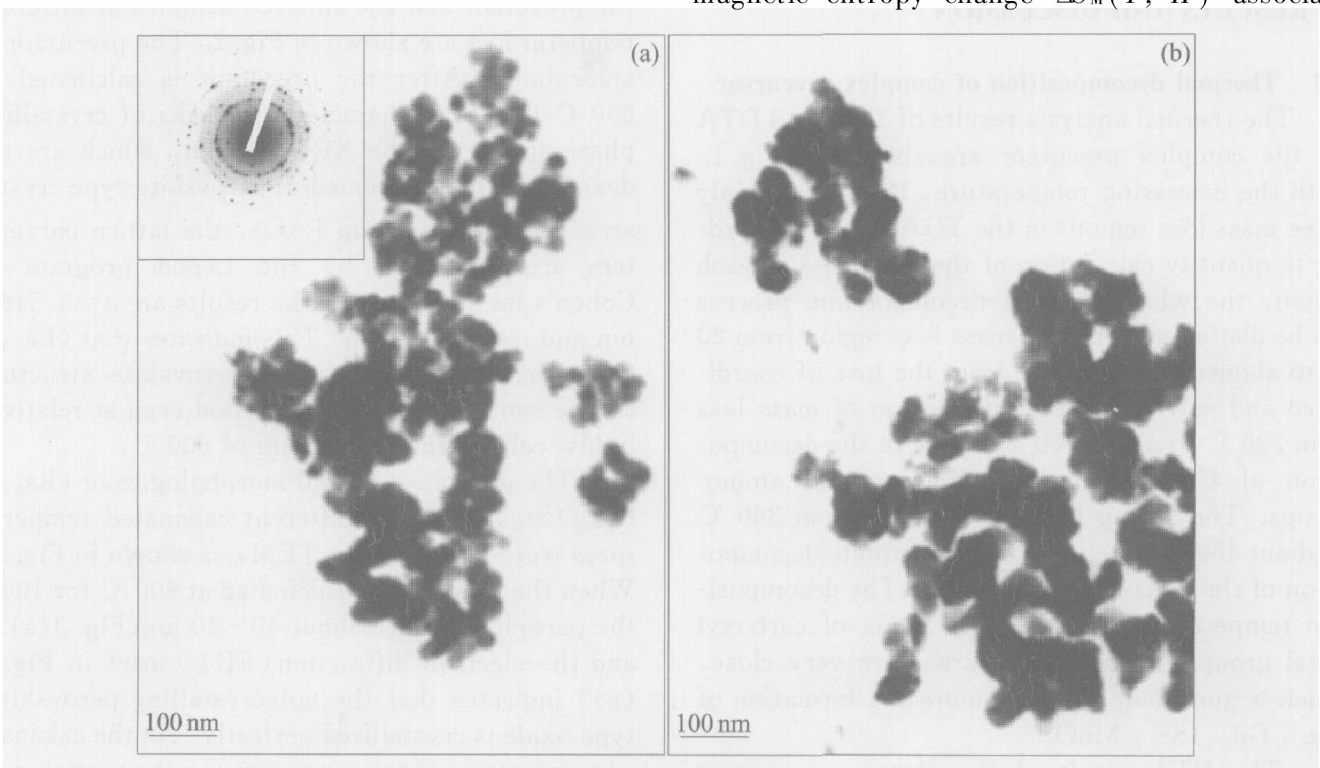

Fig. 3 TEM images of $La_{0.47}Gd_{0.2}Sr_{0.33}MnO_3$ sample at different calcinating temperatures
(a) —600 ℃, 10 h; (b) —800 ℃, 10 h

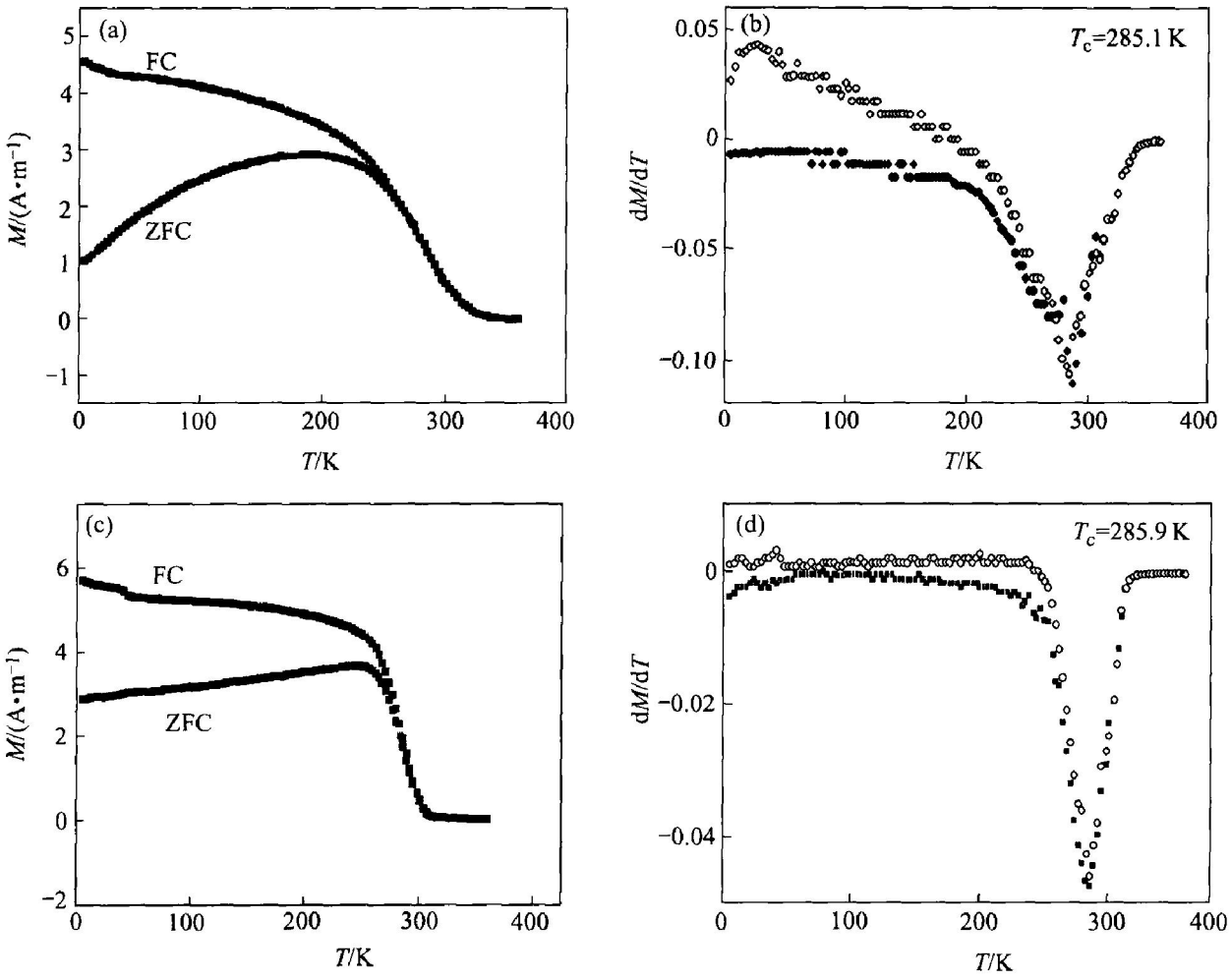

Fig. 4 Magnetization dependence of temperature in ZFC and FC process with applied field 7 957.8 A/m for $La_{0.47}Gd_{0.2}Sr_{0.33}MnO_3$ sample at different calcinating temperatures (a), (b) —600 ℃, 10 h; (c), (d) —800 ℃, 10 h

with a magnetic field variation is given by

$$\Delta S_M(T, H) = S_M(T, H) - S_M(T, 0) = \int_0^H \left|\frac{\partial M}{\partial T}\right|_H dH \quad (1)$$

In the case of magnetization measurements at small discrete field and temperature intervals, $-\Delta S_M$ can be approximated to be[28]

$$|\Delta S_M| = \sum_i \frac{M_i - M_{i+1}}{T_{i+1} - T_i} \Delta H_i \quad (2)$$

where M_i and M_{i+1} are the experimental values of the magnetization at temperature T_i and T_{i+1}. respectively, under an applied magnetic field H by measuring the isothermal M —H curve at various temperatures, one can calculate the magnetic entropy change associated with the magnetic field variation from Eqn. (2).

Fig. 5 shows the isothermal magnetization curves of nanosized $(La_{0.47}Gd_{0.2})Sr_{0.33}MnO_3$ subjected to the calcinated temperature of 600 ℃ and 800 ℃, respectively. The corresponding magnetic entropy change $-\Delta S_M$ calculated from Eqn. (2), is plotted in Fig. 6. According to Eqn. (1), the maximum of magnetic entropy change is located at T_c, where the variation of magnetization with temperature is the fastest. In our experiments, the maximum entropy change $-\Delta S_{Mmax}$ exhibits a broad peak, and the values are about 2.02 J/(kg · K^{-1}) and 3.90 J/(kg · K^{-1}) at 5 T magnetic field for the samples calcinated at 600 ℃ and 800 ℃, respectively. The magnetization and MCE for the sample calcinated at 600 ℃ is obviously lower than that for the sample calcinated at 800 ℃. In general, each particle can be seen as being composed of two different parts. The inner part is a core where double exchange interaction dominates and promotes ferromagnetic behavior. The outer part is a layer where magnetic interactions are clearly modified by defects, vacancies, stress, and broken bonds directing to a disordered magnetic state[29-31]. The cationic vacancies and the defects in the structure are mainly located in this external zone, and lead to a reduction of ferromagnetic interaction. This result indicates that high-temperature and long-time heat treatment are needed to improve the MCE in the sample synthesized from amorphous complex precursor. However, the broader peak temperature range of the magnetic entropy change around the Curie temperature probably reveals the presence of

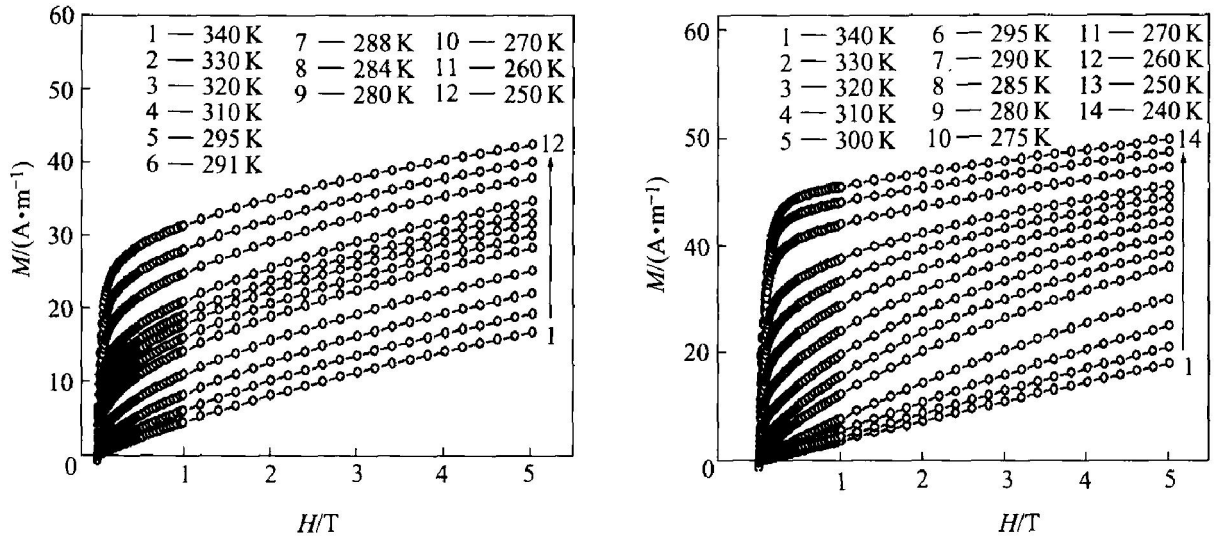

Fig. 5 M —H Curves for $La_{0.47}Gd_{0.2}Sr_{0.33}MnO_3$ sample at different calcinating temperatures
(a) —600 ℃, 10 h; (b) —800 ℃, 10 h

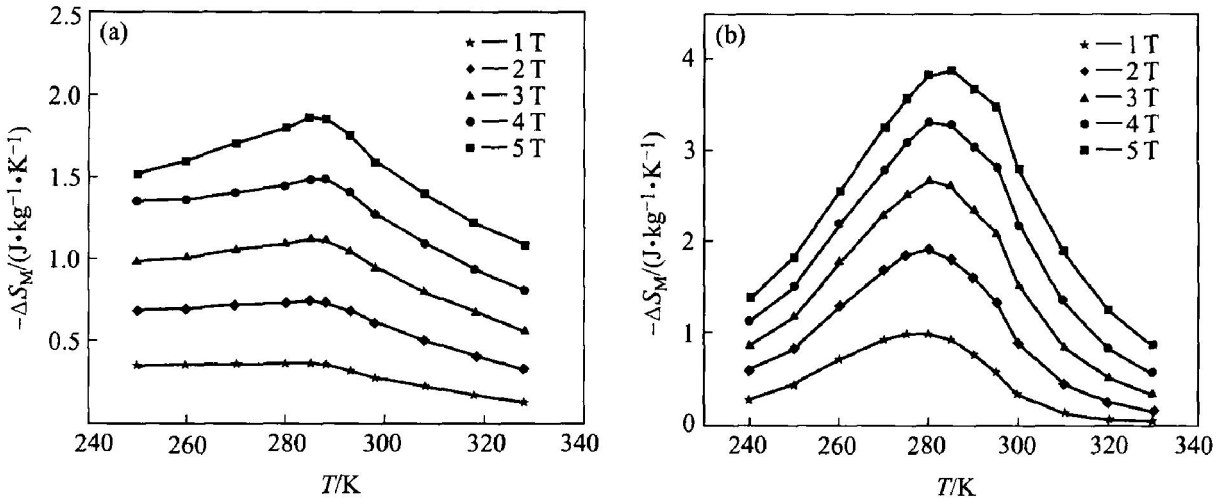

Fig. 6 Temperature dependence of $-\Delta S_M$ under 0 T to 5 T for $(La_{0.47}Gd_{0.2})Sr_{0.33}MnO_3$ sample at different calcinating temperatures
(a) —600 ℃, 10 h; (b) —800 ℃, 10 h

a distribution in magnetic exchange interactions[32].

This is a very interesting result, because we are able to change the MCE and the width of peak temperature range of the material by changing the particle size, and may select optimization, which is desirable for an Ericsson-cycle magnetic refrigeration and heat exchange technology. Therefore, it suggests that the material is a suitable candidate for magnetic refrigeration near room temperature.

4 CONCLUSIONS

1) The nanosized $(La_{0.47}Gd_{0.2})Sr_{0.33}MnO_3$ with rhombohedral structure and stoichiometry is successfully prepared at relatively low calcinating temperature of 600 ℃ and 800 ℃ for 10 h using the amorphous complex precursor. The particle sizes are 40 – 50 nm and 80 – 100 nm, respectively, and it can be controlled by varying calcinating temperature. It is an effective method to synthesize nanosized perovskite-type complex oxides.

2) There exists a large magnetic entropy change with a broad peak around the ferromagnetic-paramagnetic transition temperature (285. 9 K) for the sample calcinated at 800 ℃ for 10 h. Nanosized $(La_{0.47}Gd_{0.2})Sr_{0.33}MnO$ could be a suitable candidate as working substance in magnetic refrigeration technology near room temperature.

REFERENCES

[1] Jonker G H, Van Santen J H. Ferromagnetic compounds of manganese with perovskite structure [J]. Physica, 1950, 16: 337 – 349.

[2] von Helmolt R, Wecker J, Holzapfel B, et al. Giant negative magnetoresistance in perovskitelike $La_{2/3}Ba_{1/3}MnO_x$ ferromagnetic films [J]. Phys Rev Lett, 1993, 71: 2331 – 2333.

[3] Jin S, Tiefel T H, McCormack M, et al. Thousandfold change in resistivity in magnetoresistive La-Ca-Mn-O films [J]. Science, 1994, 264: 413 - 415.

[4] Sun Y, Salamon M B, Tong W, et al. Magnetism, electronic transport, and colossal magnetoresistance of $(La_{0.7-X}Gd_X)Sr_{0.3}MnO_3$ ($0 \leqslant X \leqslant 0.6$) [J]. Phys Rev B, 2002, 66: 094414 - 094419.

[5] Bose T K, Chahine R, Gopal B R, et al. Magnetocaloric properties of the $La_{0.7-X}Y_XSr_{0.3}MnO_3$ giant magnetoresistance ceramics [J]. Cryogenics, 1998, 38: 849 - 851.

[6] Guo Z B, Du Y W, Zhu J S, et al. Large magnetic entropy change in $La_{0.75}Ca_{0.25}MnO_3$ [J]. Phys Rev Lett, 1997, 78: 1142 - 1145.

[7] Bohigas X, Tejada J, Marinez-Sarrion M L, et al. Magnetic and calorimetric measurements on the magnetocaloric effect in $La_{0.6}Ca_{0.4}MnO_3$ [J]. J Magn Magn Mater, 2000, 208: 85 - 92.

[8] Tang T, Gu K M, Cao Q Q, et al. Magnetocaloric properties of Ag-substituted perovskite-type manganites [J]. J Magn Magn Mater, 2000, 222: 110 - 114.

[9] Sun Y, Xu X J, Zhang Y H. Large magnetic entropy change in the colossal magnetoresistance material $La_{2/3}$-$Ca_{1/3}MnO_3$ [J]. J Magn Magn Mater, 2000, 219: 183 - 185.

[10] Szewczyk A, Szymczak H, Wisnieski A, et al. Magnetocaloric effect in $La_{1-X}Sr_XMnO_3$ for $X = 0.13$ and 0.16 [J]. Appl Phys Lett, 2000, 77: 1026 - 1028.

[11] Wang Z M, Ni G, Xu Q Y, et al. Magnetic entropy change in perovskite manganites $La_{0.65}Nd_{0.05}Ca_{0.3}$-$Mn_{0.9}B_{0.1}O_3$ (B= Mn, Cr, Fe) [J]. J Magn Magn Mater, 2001, 234: 371 - 374.

[12] Yu M H, Sujatha D P, Lewis L H, et al. Novel synthesis and magnetocaloric assessment of functional oxide [J]. J Mater Sci Engineering B, 2003, 97: 245 - 250.

[13] Sun Y, Tong W, Liu N, et al. Magnetocaloric effect in polycrystalline $(La_{0.5}Gd_{0.2})Sr_{0.3}MnO_3$ [J]. J Magn Magn Mater, 2002, 238: 25 - 28.

[14] Chen H Y, Lin C, Dai D S. Magnetocaloric effect in $(La, R)_{2/3}Ca_{1/3}MnO_3$ (R= Gd, Dy, Tb, Ce) [J]. J Magn Magn Mater, 2003, 257: 254 - 257.

[15] Phan M H, Tian S B, Hoang D Q, et al. Large magnetic-entropy change above 300 K in CMR materials [J]. J Magn Magn Mater, 2003, 258 - 259: 309 - 311.

[16] Chau N, Niem P Q, Nhat H N, et al. Influence of Cu substitution for Mn on the structure, magnetic, magnetocaloric and magnetoresistance properties of $La_{0.7}Sr_{0.3}MnO_3$ perovskites [J]. Physica B, 2003, 327: 214 - 217.

[17] Gschneidner K A Jr, Pecharsky V K. Magnetocaloric materials [J]. Ann Rev Mater Sci, 2000, 30: 387 - 392.

[18] Gschneidner K A Jr, Pecharsky V K. Magnetic refrigeration materials [J]. J Appl Phys, 1999, 85: 5365 - 5368.

[19] Rao C N R, Mahesh R, Raychaudhuri A K, et al. Giant magnetoresistance, charge ordering and other novel properties of perovskite manganates [J]. J Phys Chem Solids, 1998, 59: 487 - 502.

[20] Zhang N, Yu Z Q, Xing D Y, et al. Spin-polariztion dependent carrier diffusion study of CMR effect in manganese perovskite [J]. Phys Lett A, 2002, 297: 446 - 553.

[21] Hwang H Y, Cheong S W, Ong N P, et al. Spin-polarized intergrain tunneling in $La_{2/3}Sr_{1/3}MnO_3$ [J]. Phys Rev Lett, 1996, 77: 2041 - 2044.

[22] McMichael R D, Ritter J J, Shull R D. Enhanced magnetocaloric effect in $Gd_3Ga_{5-X}Fe_XO_{12}$ [J]. J Appl Phys, 1993, 73: 6949 - 6951.

[23] Yamamoto T A, Tanaka M, Misaka Y, et al. Dependence of the magnetocaloric effect in superparamagnetic nanocomposites on the distribution of magnetic moment size [J]. Scripta Materialia, 2002, 46: 89 - 94.

[24] Sanchez R D, Rivas J, Vazquez C V, et al. Giant magnetoresistance in fine particle of $La_{0.67}Ca_{0.33}MnO_3$ synthesized at low temperatures [J]. Appl Phys Lett, 1996, 68: 134 - 136.

[25] Vazquez C V, Blanco M C, Quintela M A L, et al. Characterization of $La_{0.67}Ca_{0.33}MnO_{3\pm\delta}$ particles prepared by the sol-gel route [J]. J Mater Chem, 1998, 8: 991 - 1000.

[26] Langford J I. Powder pattern programs [J]. J Appl Crystall, 1971, 4: 259 - 276.

[27] Hashimoto T, Numasawa T, Shino M, et al. Magnetic refrigeration in the temperature range from 10 K to room temperature: the ferromagnetic refrigerants [J]. Cryogenics, 1981, 21: 647 - 653.

[28] Foldeaki M, Chahine R, Bose T K. Magnetic measurements: a powerful tool in magnetic refrigerator design [J]. J Appl Phys, 1995, 77: 3528 - 3537.

[29] Coey J M D. Noncollinear spin arrangement in ultrafine ferrimagnetic crystallites [J]. Phys Rev Lett, 1971, 27: 1140 - 1142.

[30] Kodama R H, Berkowitz A E, MeNiff E J, et al. Surface spin disorder in $NiFe_2O_4$ nanoparticles [J]. Phys Rev Lett, 1996, 77: 394 - 397.

[31] Park J H, Vescovo E, Kim H J, et al. Magnetic properties at surface boundary of a half-metallic ferromagnet $La_{0.7}Sr_{0.3}MnO_3$ [J]. Phys Rev Lett, 1998, 81: 1953 - 1956.

[32] Gallagher K A, Willard M A, Zabenkin V N, et al. Distributed exchange interactions and temperature dependent magnetization in amorphous $Fe_{0.88-X}$-$Co_XZr_7B_4Cu_1$ alloys [J]. J Appl Phys, 1999, 85: 5130 - 5132.

(Edited by LI Xiang-qun)